Journal of the European Ceramic Society 22 (2002) 1501–1512

www.elsevier.com/locate/jeurceramsoc

Microstructural evolution under load and high temperature deformation mechanisms of a mullite/alumina fibre

F. Deléglise, M.H. Berger*, A.R. Bunsell

Ecole des Mines de Paris, Centre des Matériaux, BP 87, Evry Cedex, France

Received 31 May 2001; received in revised form 22 August 2001; accepted 19 September 2001

Abstract

A two-phase mullite alumina fibre, the 3M Nextel 720 fibre, has been studied in tension and creep. The fibre shows the highest creep resistance of all current commercial fine oxide fibres up to 1500 °C. The creep mechanisms involve progressive dissolution of mullite and simultaneous reprecipitation of alumina into elongated oriented grains and grain boundary sliding by a thin aluminosilicate liquid phase. The rate of grain growth in creep at a given temperature is dependant on the applied stress. The combination of sub-micron size mullite crystallites and alumina grains gives rise to a high sensitivity to alkaline contamination. Stress enhanced diffusion of the contaminants from the fibre surface results in crack nucleation, dissolution of mullite, formation of a liquid phase and slow crack growth. From 1200 °C, this process is coupled with a fast α-alumina grain growth at the fibre surface.

Keywords: Al_2O_3; Creep; Fibres; Microstructure; Mullite

1. Introduction

The development of ceramic matrix composites capable of operating at high temperatures above 1100 °C in air, requires fibre reinforcements which are stable under thermomechanical loading conditions in oxidative environments. Oxide based fibres do offer the possibility of long term use in air at high temperature. However, at temperatures above around 1000 °C single phase polycrystalline alumina fibres have been found to suffer from creep and the weakening of grain boundaries results in major strength loss.[1] The mullite/alumina Nextel 720 fibre is one of the latest of a series of fibres produced by Minnesota Mining and Manufacturing (3M) based on alumina or mullite. The manufacturer claims a reduced creep rate of three orders of magnitude compared to that of a single phase polycrystalline alumina Nextel 610 fibre and attributes this improvement to the two-phase microstructure consisting of mosaic and elongated grains.[2] The complexity of the crystal structure of mullite and the presence of mosaic grains acting as single larger entities[3] are expected to reduce the creep rates of this fibre. These assumptions make the Nextel 720 a good candidate for reinforcement in high temperature ceramic matrix composites. The aim of this paper is to determine the microstructural evolution occurring under load at high temperatures of a mullite/alpha-alumina system and the related deformation mechanisms, damage and failure modes.

2. Experimental details

The external surfaces of the fibres as well as their fracture surfaces were observed using a LEO DSM 982 Gemini field emission gun scanning electron microscope at acceleration voltages between 1 and 3 kV. The microstructures were investigated using a PHILIPS EM 430 transmission electron microscope with an acceleration voltage of 300 kV. Thin foils were obtained using a method described elsewhere.[4] Heat treatments were performed in a $MoSi_2$ resistance oven. An X-ray diffractometer Siemens D500 was used to analyze the evolution of different phases after high temperature loading. The radiation corresponded to the $K_{\alpha 1}$ line of cobalt ($\lambda = 0.1789$ nm). Semi-quantitative microanalysis

* Corresponding author.
E-mail address: marie-helene.berger@mat.ensmp.fr (M.H. Berger).

0955-2219/02/$ - see front matter
PII: S0955-2219(01)00461-7

was performed using energy dispersive X-ray spectroscopy in TEM.

Single filaments and bundles of fibres were tested in tension and creep up to 1500 °C on two horizontal tensile machines with a maximum displacement speed of 1.5 mm/s and force sensitivities of 10^{-2} N for single fibres and 0.5 N for bundles.[5] The diameters of the fibres were measured prior to each test on single fibres using a Watson image shearing eyepiece mounted on an optical microscope giving an accuracy of 0.5 μm.[5] The number of fibres loaded in the bundle was estimated from the slope of an initial partial tensile load versus displacement curve at room temperature, knowing the value of the Young's modulus of a monofilament and by subtracting the compliance of the tensile machine. The accuracy evaluating the number of fibres loaded was better than 90%. The failure or applied stresses were then determined with a precision of 10% for single fibres and 17% for bundles. A resistance oven composed of a lanthanum chromite heating element placed around an alumina inner tube allowed the fibres to be tested at high temperatures with extremely rapid heat-up rates. The grips remained cold and the hottest part of the furnace was 25 mm long with ±25 °C for single filaments and 40 mm with ±25 °C for bundles. Additional tensile tests were performed with a platinum furnace to investigate a possible contamination by the heating elements of the furnaces used.

Great care was taken not to contaminate the fibres during handling. Contact with the skin was avoided by the use of surgical gloves.

3. As received fibre and thermal stability

The Nextel 720 mullite-alumina fibre is produced using a sol-gel route with a diameter of 12.5 μm and is composed of 85% Al_2O_3 and 15% SiO_2 by weight. The room temperature single filament strength announced by the manufacturer is 2100 MPa for a gauge length of 25 mm and its Young's modulus is 260 GPa.[2] Previous studies[3] have revealed that the fibre exhibits linear elastic behaviour at room temperature with brittle failure, which is most often initiated from a surface defect. Fracture morphologies are flat as can be seen in Fig. 1, no faceted grains can be observed but the failure surfaces show a roughness at a sub-micron scale.

The fibre consists of 60% of an alumina rich (2:1) mullite and 40% α-alumina by weight with around 4% porosity. [3] Its microstructure, shown in Fig. 2, is a continuum of mosaic grains of pseudo-tetragonal (2:1) mullite with wavy contours and with an average size of 500 nm. These mosaic grains consist of clusters of grains of a few tens of nanometers, each grain being slightly disorientated with respect the other grains of the cluster. They enclose some round or elongated α-alumina grains of an average size between 50 and 100 nm. Elongated grains have aspect ratios of up to 6, the [0001] direction of α-alumina being normal to the elongated axis of the

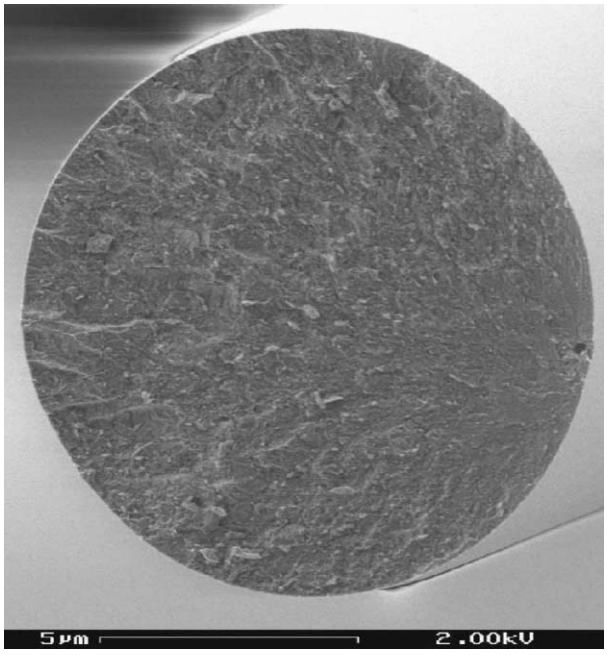

Fig. 1. Fracture morphology of Nextel 720 fibre at room temperature. Failure was initiated from a void near the fibre surface.

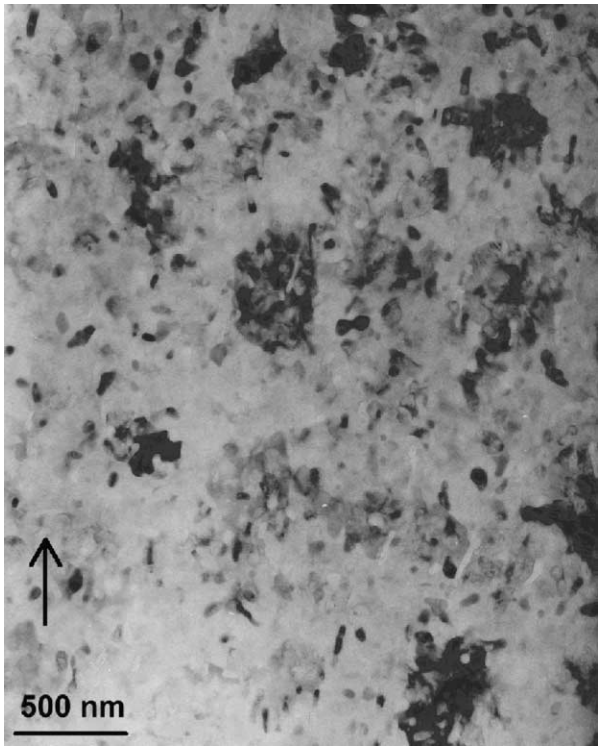

Fig. 2. Microstructure of as received Nextel 720 fibre made of mullite mosaic grains with irregular contours containing spherical and elongated alpha alumina particles. The elongated particles are preferentially aligned in the fibre axis direction (arrowhead).

grains. These elongated alumina grains show a preferential orientation with respect to the fibre axis direction. No amorphous intergranular phase was revealed by TEM and high resolution TEM in the as received fibre.

Chemical data given by the manufacturer indicate that the fibre contains 0.3% Fe as a nucleating agent for the formation of α-alumina and a few ppm of Na, K and Cl in the bulk of the fibre.[2] In addition it has been shown that the fibres used for the previous and present studies present randomly distributed areas of a few microns on their surfaces which are richer in Ca, Na, Mg and Cl and K and depleted in oxygen, compared to the rest of the fibre surface and core.[3]

Heat treatments of the Nextel 720 fibre from 1300 °C provoke a rearrangement of the microstructure which evolves towards a recrystallisation of the (2:1) mullite aggregates into facetted (3:2) mullite grains and oriented elongated α-alumina grains with a bimodal distribution.[3,6,7] After 3 h at 1300 °C, α-alumina platelet grains of 0.5 μm were observed locally on the fibre surface in circular zones of a few microns. [3] After 84 h at 1500 °C the fibre core shows α-alumina grains of up to 5 μm in size.

4. High temperature mechanical behaviour

4.1. Tensile behaviour

4.1.1. Tensile strength at high temperature

The tensile strengths as a function of the stressing rate of single filaments were measured from room temperature up to 1200 °C. In this temperature range no measurable plasticity was observed within the resolution of the LVDT. The fibre strength was almost constant up to 1000 °C and was independent of the stressing rate in the range of 15–1000 MPa/s. From 1100 °C the failure stress decreased rapidly as shown in Fig. 3 with a more pronounced fall at the lowest stressing rates.

The variations of fibre strength σ as a function of the stressing rate, $\dot{\sigma}$, at temperatures of 1100 and 1200 °C are shown in Fig. 4. The slow crack velocity V can be expressed as a power function of the stress intensity factor K_I: $V = A \cdot K_I^N$ where A and N are constants for a given temperature.[8] The exponent N was calculated from the expression

$$\log \sigma = \log B + [1/(N+1)] \log \dot{\sigma}$$

where B is a constant at a given temperature. [8] The calculated N values were equal to 10 and 5 at 1100 and 1200 °C, respectively.

4.1.2. Fracture morphology

The single fibre primary fracture surfaces had similar appearances up to 1000 °C as those at room temperature. The fracture surfaces of the fibres tested at 1200 °C were drastically different. At the lowest stressing rates, grains of a few microns in size and in the form of platelets had developed on the external fibre surface (Fig. 5a). The platelets were identified using EDS analysis and TEM as being of α-alumina. At higher stressing rates (100 MPa/s), these large grains were embedded in a glassy silicate phase as shown in Fig. 5c. At 1000 MPa/s the size of the alumina grains decreased but the amount of silicate phase formed increased (Fig. 5d). Chemical analysis in these regions showed the presence of contaminants, the most frequent being calcium or sodium but no chromium or lanthanum was detected.

Fibres heated to 1200 °C for 5 h in the tensile machine, but without an applied load, showed very little change in strength at room temperature and did not reveal abnormal grain growth. Fibres loaded at 1200 °C at 15 MPa/s up to 90% of the failure load were also observed in SEM and no abnormal surface grain growth was detected. The growth of the alumina platelets under load occurred in the last 2 s of the test with a growth rate of the order of 1 μm/s. In the images shown in Fig. 5 an intergranular fracture area can be seen to have fanned out symmetrically from these large grains followed by an intragranular failure zone. The relative

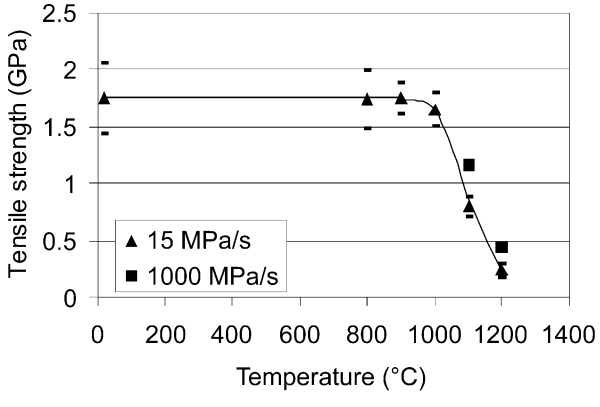

Fig. 3. Temperature dependence of the tensile strength.

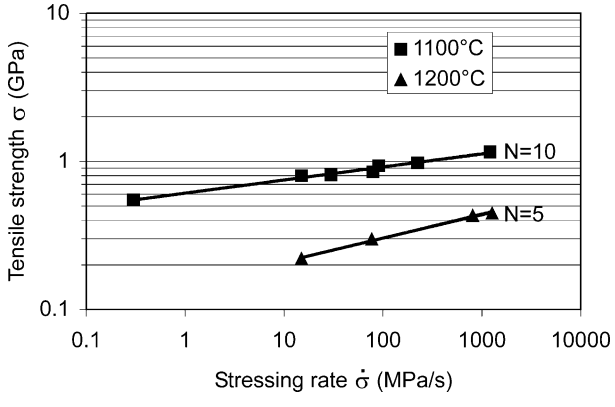

Fig. 4. Variation of the tensile strength (σ) as a function of stressing rate ($\dot{\sigma}$).

sizes of theses two zones depended on the stress rate and on the tensile strength. Fig. 5a, c and d illustrate that the size of the zone of slower intergranular failure increased with decreasing stress rates and tensile strengths. Fibres loaded at 1100 °C did not systematically show exaggerated grain growth at the surface but their failure surface presented two propagation modes as at 1200 °C, the respective size of which depended on the stressing rates.

4.1.3. Influence of the experimental environment

As an influence of external contaminants on the high temperature fibre strength was suspected, additional tensile tests were performed in a platinum heating element furnace on single filaments and in the $LaCrO_3$ furnace on bundles of fibres.

The strength from 1100 °C measured in the platinum furnace at the same stressing rates as previously used, were found to be around 1.5 times higher than those measured when tested in the $LaCrO_3$ heating element furnace. The fracture surfaces of single fibres broken in the platinum furnace presented similar features as those broken in the $LaCrO_3$ furnace: the α-alumina platelets were present as well as the glassy phase but their growth required higher loads than in the $LaCrO_3$ furnace. The sizes of intragranular and intergranular propagation zones were also found to be dependent on the stressing rates in the same way. Tensile tests performed at 1200 °C on bundles of fibres, in a $LaCrO_3$ furnace, gave two distinct fibre fracture morphologies. The fibres on the outside of a bundle presented the same defects as did single fibres tested at these temperatures. However, the fracture surfaces of the fibres contained inside the tested bundles presented no abnormal grain growth and had the same appearance of that of monofilaments broken at room temperature.

4.2. Creep behaviour

Single fibres stressed to 50 and 200 MPa at 1200 °C failed after 7 and 3 min respectively, and exhibited similar fracture morphologies to those tested in tension at 1200 °C. Tensile creep tests were then performed on bundles of fibres at temperatures between 1200 and 1500 °C with stresses ranging from 5 to 380 MPa. Bundles were used to avoid exaggerated grain growth at the surfaces of the majority of the fibres and premature

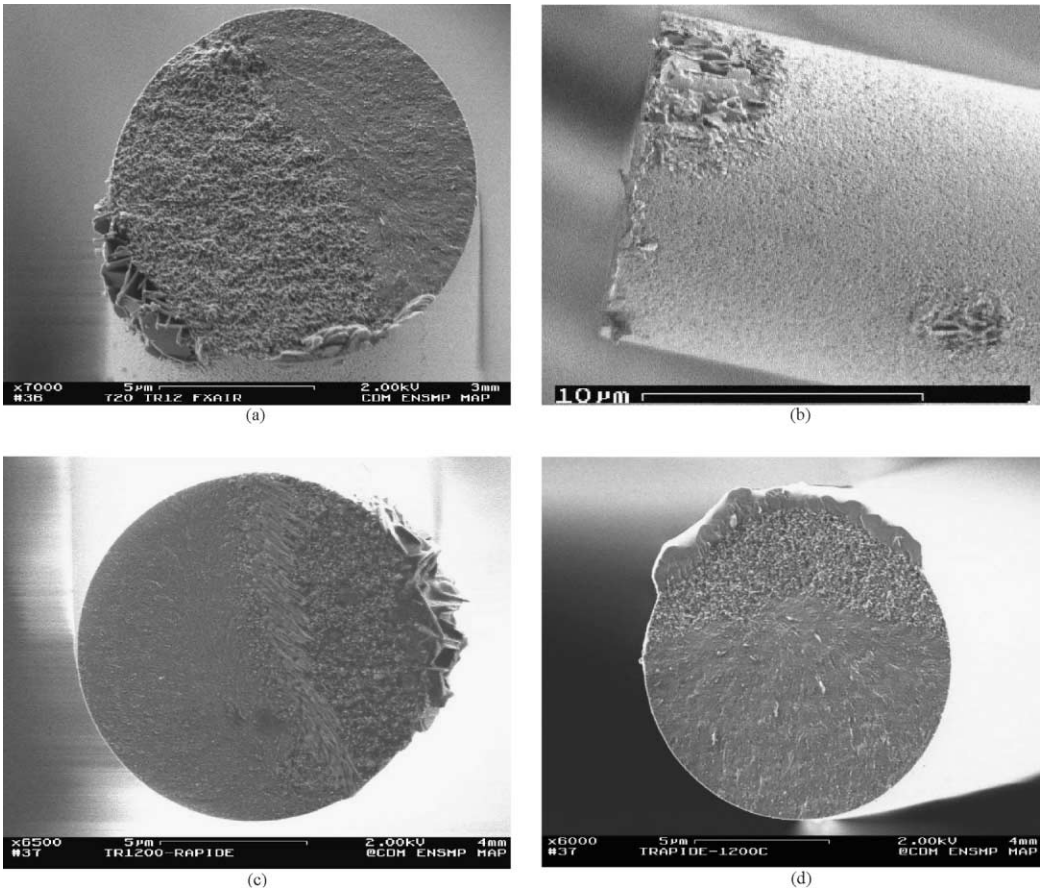

Fig. 5. Appearance of single fibres tested in tension at 1200 °C in air. (a) Failure surface obtained with a stressing rate of 15 MPa/s. (b) Fibre surface below the failure surface showing circular zones containing alumina platelet grains, one of which has led to fibre failure. (c) Fibre fracture surface obtained with a stressing rate of 100 MPa/s. Alumina platelets are surrounded by a silicate phase. (d) Fibre fracture surface obtained with a stressing rate of 1000 MPa/s. The amount of silicate phase increased and the alumina grain size decreased compared to (a) and (c).

failure during primary creep. Fig. 6 a and b shows typical creep curves obtained at 1300 and 1500 °C and steady-state creep rates as a function of the applied stresses are shown in Fig. 7. Fig. 8 reveals the evolution of the microstructure during creep and Fig. 9 shows fracture morphologies and surface features after failure in creep. Fig. 10 summarises the creep behaviour from 1200 up to 1500 °C as a function of the applied stress.

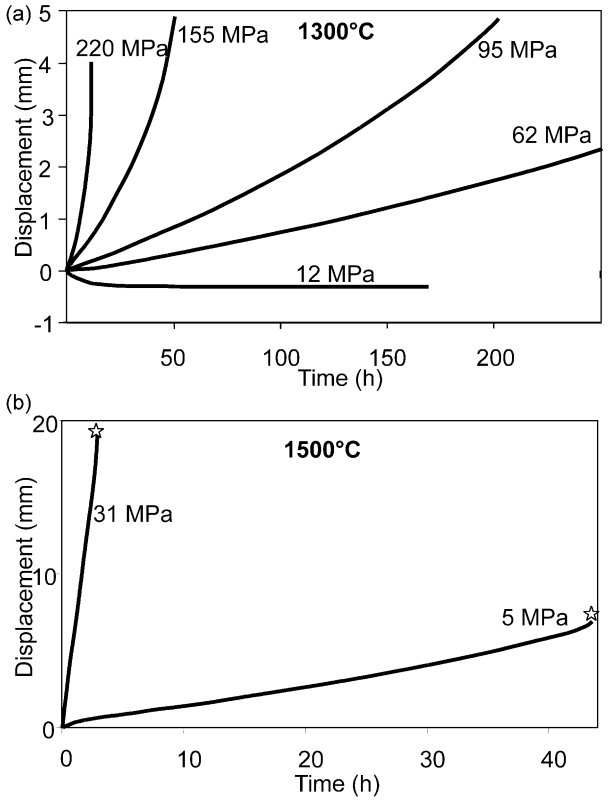

Fig. 6. Creep curves obtained with bundles of fibres (a) at 1300 °C and (b) at 1500 °C.

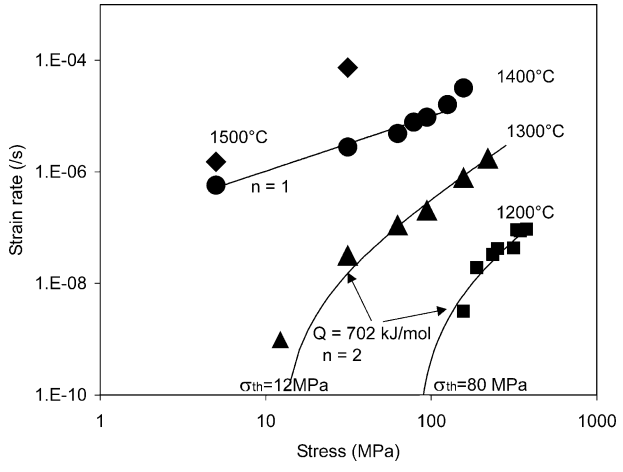

Fig. 7. Strain rate as a function of applied stress at temperatures from 1200 to 1500 °C.

At 1200 and 1300 °C the creep curves could be classified into three stress regions:

- At the lowest applied stresses up to 80 MPa at 1200 °C and 12 MPa at 1300 °C the Nextel 720 fibre exhibited only negative deformation (shrinkage).
- For intermediate stress levels, up to 160 MPa at 1200 °C and 62 MPa at 1300 °C, the creep curves presented an initial region of shrinkage, followed by positive deformation. For these low and intermediate stress levels, the creep tests were stopped after 10 days without reaching the failure of the bundles. A slight increase in the grain growth rate was noticed compared to fibres heat treated for 10 days without load, with the development of elongated alpha alumina grains.
- At the highest stresses the fibre showed only positive deformation and damage accumulated by the development of intergranular microcracks. Crack propagation was first intergranular and non planar. Catastrophic intragranular failure occurred when the remaining cross section could no longer carry the applied load and this gave rise to a failure surface divided into a non planar intergranular zone and a planar intragranular zone, as can be seen in Fig. 9a. Fig. 9a further reveals a significant grain growth in the intergranular zone whereas below the failure surface, TEM observations showed only slight microstructural evolution which was very similar to that obtained without load after heat treatment at the same temperature and for the same duration.

At 1400 °C three stress regions have been identified:

- At the lowest stresses used, 5 MPa, shrinkage occurred during the first 8 h of the creep test and was then followed by positive deformation leading to the failure of the bundle after more than 75 h. The average rate of grain growth was comparable to that observed after heat treatment without load for the same time and resulted in the recrystallisation of the mullite aggregates into faceted grains and the growth of elongated alpha alumina grains. In addition to this grain growth, an abnormal growth of some elongated α-alumina grains of up to several tens of microns occurred within the fibre core region under load Fig. 8a. The long facets of these grains were oriented with respect to the load axis and corresponded to the basal plane of alpha-alumina. Failure surfaces were flat with the fracture being initiated at some isolated large grains.
- For intermediate stress levels, at 30 and 60 MPa, the fibre bundles exhibited only positive deformation and the increase in stress level led to shorter times to failure (25 and 22 h, respectively) which did not produce exaggerated growth of alumina grains. The average grain growth was still of the

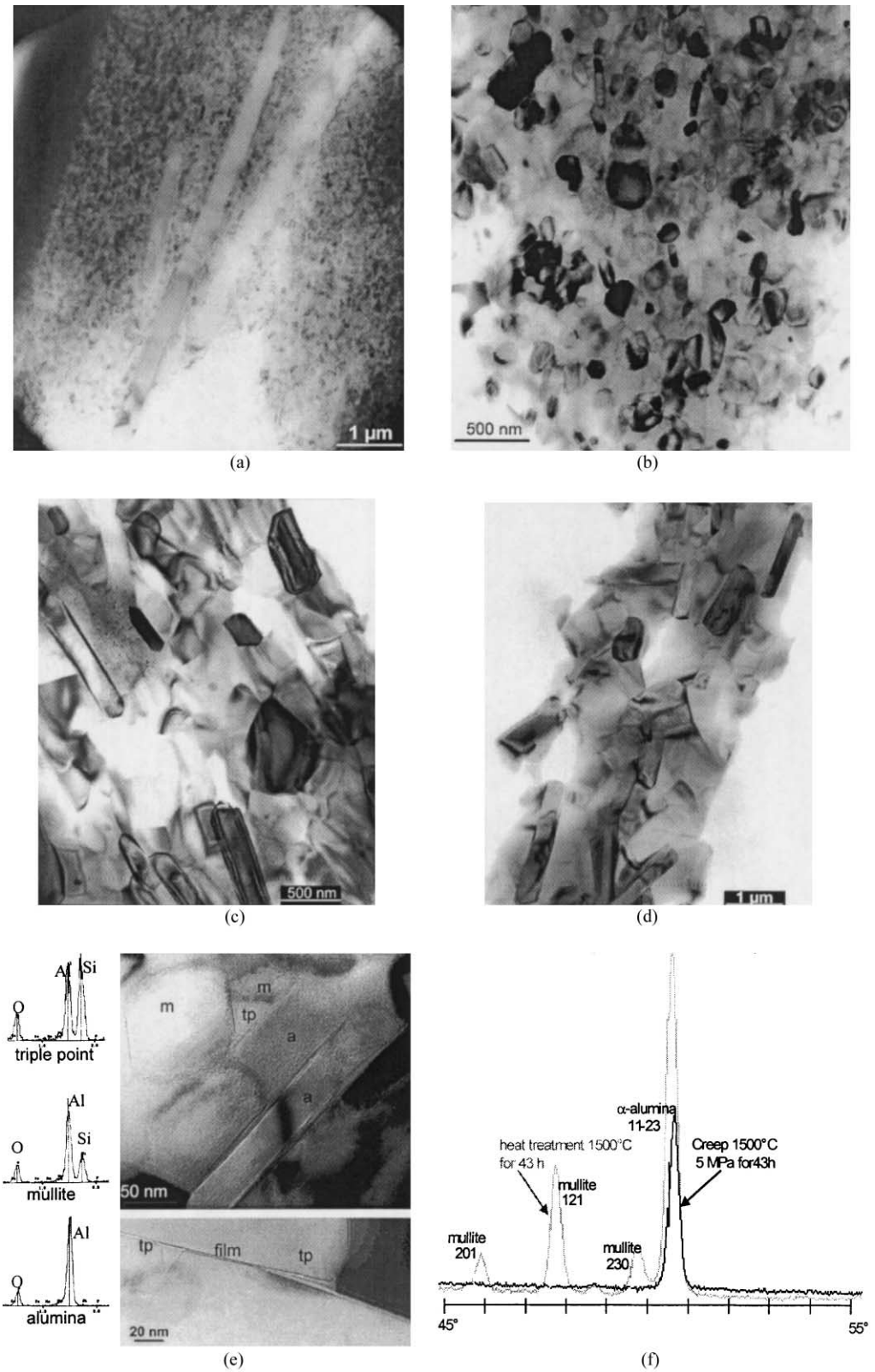

Fig. 8. Microstructural evolution in creep. (a) $T = 1400\ ^{\circ}C$, $\sigma = 5$ MPa, $t_R = 84$ h, $\varepsilon_R = 12\%$. Abnormal growth of α-alumina in the load direction. (b) $T = 1400\ ^{\circ}C$, $\sigma = 62$MPa, $t_R = 22$ h, $\varepsilon_R = 20\%$. Moderate overall growth. (c) $T = 1400\ ^{\circ}C$, $\sigma = 80$MPa, $t_R = 14$ h, $\varepsilon_R = 52\%$. Oriented growth of elongated α-alumina grains, reduction of the mullite content, presence of cavities. (d) $T = 1500\ ^{\circ}C$, $\sigma = 5$MPa, $t_R = 43$ h 30, $\varepsilon_R = 12\%$. Oriented growth of elongated α-alumina grains and an absence of mullite grains. (e) $T = 1400\ ^{\circ}C$, $\sigma = 62$ MPa, $t_R = 22$ h, $\varepsilon_R = 20\%$. Intergranular alumino-silicate films and triple points (tp) between alumina (a) and mullite (m) grains and their corresponding EDX spectra. (f) XRD spectra of the fibre after creep (black spectrum), $T = 1500\ ^{\circ}C$, $\sigma = 5$ MPa, $t_R = 43$ h 30, $\varepsilon_R = 12\%$, and after heat treatment without load for the same time and temperature (grey spectrum).

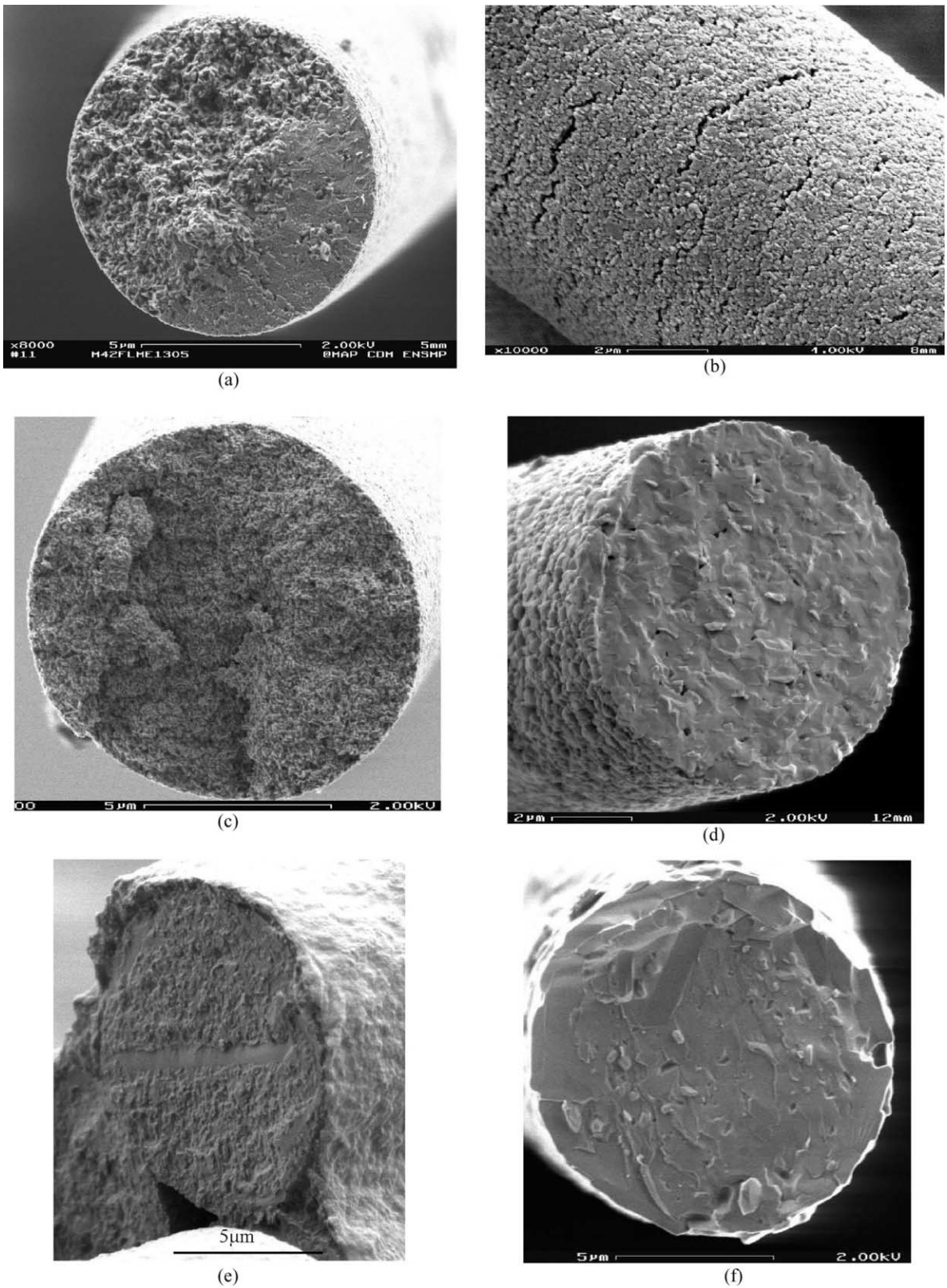

Fig. 9. Fracture morphology and fibre surface after creep. (a) $T = 1300\ ^{\circ}C$, $\sigma = 155$ MPa, $t_R = 50$ h, $\varepsilon_R = 8.6\%$. Intergranular crack propagation (upper left part) is followed by a catastrophic intragranular planar failure of the remaining section. (b) $T = 1400\ ^{\circ}C$, $\sigma = 62$ MPa, $t_R = 22$ h, $\varepsilon_R = 20\%$. The fibre surface shows intergranular microcracks and grain growth. (c) $T = 1400\ ^{\circ}C$, $\sigma = 62$ MPa, $t_R = 22$ h, $\varepsilon_R = 20\%$. The coalescence of several intergranular microcracks led to a non planar fracture. (d) $T = 1400\ ^{\circ}C$, $\sigma = 80$ MPa, $t_R = 14$ h, $\varepsilon_R = 52\%$. Planar failure surface induced by an overall grain growth and cavity formation. (e) $T = 1500\ ^{\circ}C$, $\sigma = 5$ MPa, $t_R = 43$ h 30, $\varepsilon_R = 12\%$. Abnormal growth of an alumina grain. The fibres are covered with a silicate phase. (f) $T = 1500\ ^{\circ}C$, $\sigma = 31$ MPa, $t_R = 3$ h, $\varepsilon_R = 45\%$. Planar failure surface induced by an overall grain growth and cavity formation.

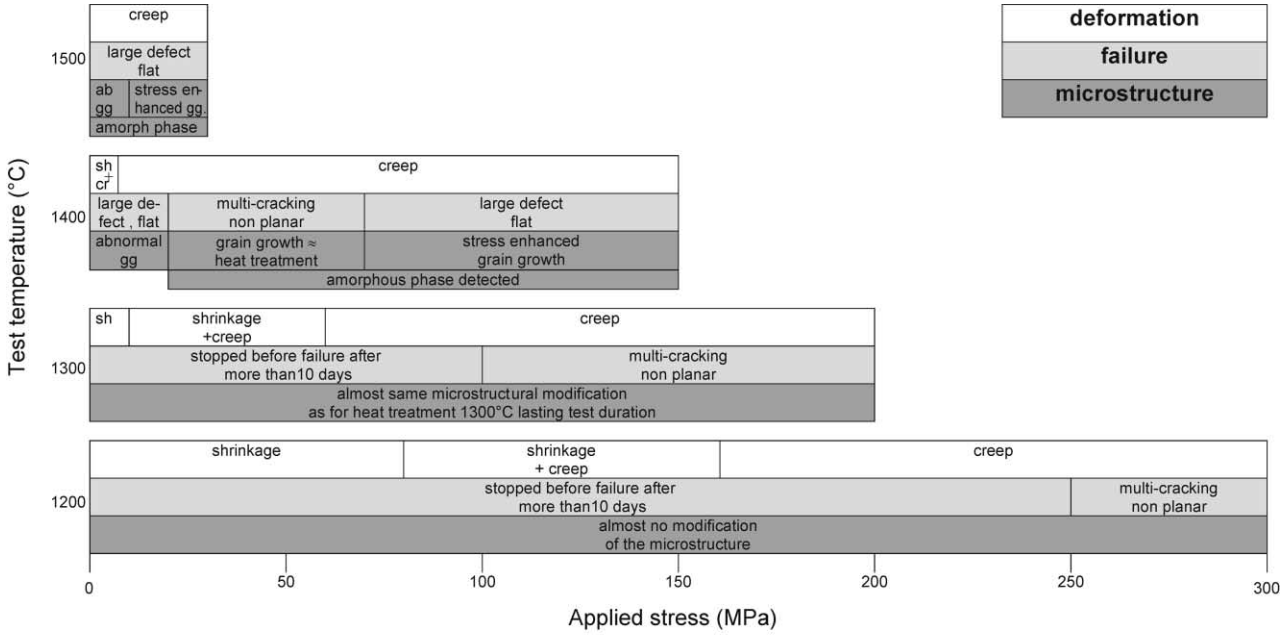

Fig. 10. Summary of the behaviour of the Nextel 720 fibre in creep from 1200 to 1500 °C as a function of the applied stress. (ab = abnormal, gg = grain growth, sh = shrinkage, cr = creep).

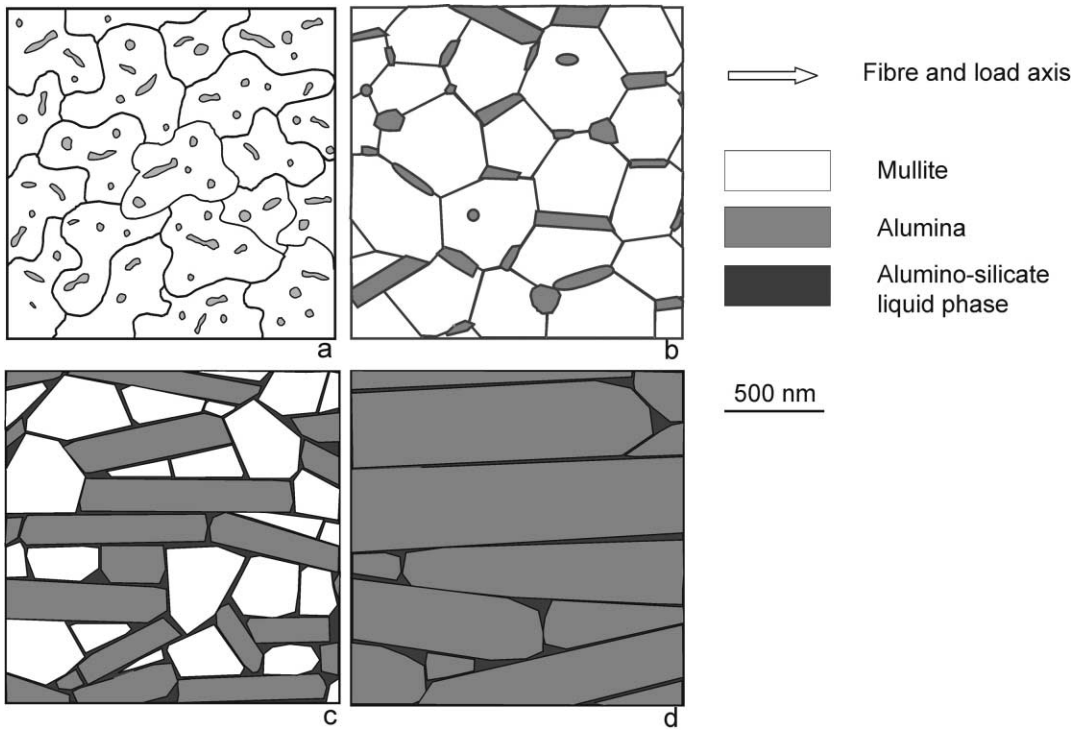

Fig. 11. Schematic diagrams of the creep mechanisms (a) As received fibre. (b) Recrystallisation of the mullite (2:1) aggregate grains into facetted (3:2) mullite grains accompanied by the rejection of the intragranular alumina particles to the outside the mullite grains and their oriented growth. Sliding of mullite and alumina grains. (c) Dissolution of mullite grains in presence of alkalis which provides an alumino-silicate liquid phase of low viscosity. The grains slide in this fluid phase which is squeezed to the outer regions of the fibres. The diffusion of aluminium ions through the liquid phase and reprecipitation of these aluminium and oxygen on alumina grains induce growth in the tensile axis direction. (d) After long term creep tests at 1500 °C the fibre is composed of elongated α-alumina grains of several microns separated by a thin silicate phase.

same order of that occurring during heat treatment for the same times and temperature but the fibres contained some silica rich amorphous pockets at triple points and showed Fresnel fringes between grain facets, as shown on Fig. 8e. The damage was induced by the development of several intergranular microcracks, as seen in Fig. 9b and fracture resulted from their coalescence as shown in Fig. 9c.

- From 80 MPa, the fractures were catastrophic and planar and were initiated by the growth of large grains or cavities, as seen in Fig. 9d. Fig. 8c shows the core of a fibre after a creep test at 80 MPa which induced the failure of the bundle after 14 h. The grain growth was more pronounced than without load and showed the formation of numerous elongated alpha alumina grains of around one micron in length occupying more than a half of the section, cavities at triple points and Fresnel fringes between grains.

At 1500 °C, no shrinkage was observed and two types of failure modes and microstructural evolution were identified:

- At 5 MPa a bundle failed after 43 h with a strain of 12%. The fibres were stuck to each other by an external silicate layer and showed abnormal grain growth of a few grains together with flat failure surfaces, as seen in Fig. 9e. The fibre cores contained almost only alpha alumina elongated grains, the majority being of around one micron in length, as seen in Fig. 8d. Mullite was not detectable by XRD analysis of the corresponding fibre bundle, as can bee seen in Fig. 8f. The Al/Si ratio of the whole section of a fibre was measured, using EDX, to be the same as that of an as-received fibre but silicon was found to be rejected to the outer silicate layer.
- At 31 MPa, the bundle failed after 3 h with a strain of 45%. The fracture morphologies were flat and exhibited elongated grains of several microns and intergranular cavities. Below the fracture surface the fibre contained elongated alumina grains of several microns as well as isotropic mullite grains and numerous amorphous pockets at triple points and Fresnel fringes between grains.

5. Discussion

5.1. Microstructural evolution under load

The microstructure of the Nextel 720 fibre consisting of irregular clusters of mullite grains enclosing nanometric alpha-alumina particles is typical of a sol-gel process with a rapid pyrolysis step. Longer heat treatments without load at 1300 °C, a temperature close to the pyrolysis temperature,[9] allows the microstructure to evolve in order to reduce interfacial energies. The microstructures of the fibres subjected to tension or creep reveal, however, a much faster rate of evolution than during heat treatments.

The abnormal growth of alumina grains perpendicular to the c-axis in a bulk alumina ceramic has been reported to take place even with very low concentrations of $CaO+SiO_2$ or Na_2O+SiO_2 co-dopants with growth rate of 10 μm/min at 1600 °C.[10] The ternary phase diagrams of Na_2O–Al_2O_3–SiO_2 and CaO–Al_2O_3–SiO_2 systems show the existence of silicate phases with melting points below 1100 °C. Thin intergranular liquid films allow a faster transport of aluminium ions than along a solid/solid interface. Moreover the anisotropic energies and different solubility of Al_2O_3 interfaces with respect to the liquid in the presence of CaO or Na_2O induce the formation of elongated platelike grains with flat boundaries along the long axis, which correspond to the basal plane as lowest energy plane.[10] Dissolution of mullite during heat treatment and high temperature loading has also been described in mullite samples doped with alkali.[11,12] This dissolution is coupled with the transport of matter through a liquid phase and mullite reprecipitation on other interfaces. Elongated alumina growth and mullite dissolution, described for these single phase systems, occur simultaneously in the mullite/alumina system studied. The higher rate of microstructural modification observed in the fibre, compared to the single phase materials, shows a synergistic relationship with this two phase nanostructure.

Liquid silicate phases are formed in this mullite alumina fibre under load, from at least 1100 °C, by the dissolution of mullite in the presence of contaminants such as Ca or Na. The dissolution of mullite produces an alumino-silicate liquid phase the viscosity of which is lowered, compared to that of silica, by the presence of aluminium, calcium and sodium. Aluminium and oxygen ions in this liquid phase are consumed preferentially so as to redeposit on α-alumina elongated grains. This leads to an enrichment in silicon of the liquid phase and shifts the equilibrium between mullite and the melt towards the dissolution of mullite so that the mullite exsolution rate is higher than in mullite samples in the absence of alumina particles.

In the presence of an additional alkali contamination from the experimental environment, rapid alumina growth can occur under load from 1200 °C. Platelet grains grew during the last 2 s of the tensile test as there were not detected in tests stopped at around 90% of the failure stress ($\sigma_R = 240$ MPa) at a stressing rate of 15 MPa/s. Exaggerated growth was seen at lower loads but required longer times, for example fibres subjected to a constant load corresponding to 20% of failure stress failed after seven minutes showing similar platelet grains. This grain growth is enhanced by the stress and was not seen, without load, after 5 h at 1200 °C in the

same furnace. It is initiated around preexisting surface flaws or voids, in a locally alkaline rich chemical heterogeneity on the fibre surface and, during tensile tests, at a stress threshold which depends on the external contamination provided by the environment. The tensile load parallel to the fibre surface permits faster transport of the contaminant elements by surface diffusion on the preexisiting flaws or pores and surface reactions.[13] This induces the nucleation of a crack and also increases the mullite dissolution rate in the near surface of the fibre so allowing fast alumina grain growth by liquid transport. Under these conditions, the alumina growth rate at 1200 °C is of the order of 1 μm/s which is 6 times higher than those reported for α-alumina doped with CaO and SiO_2 at 1600 °C.[10]

In parallel, the nucleated crack propagates by a slow intergranular growth process. The elongated alumina growth, which is confined to this intergranular propagation zone of the failure surface, indicates the formation of an intergranular liquid phase around the crack tip by surface reaction, allowing local relaxation of the stress and subcritical crack growth even if the bulk of the fibre deforms elastically.[13] As the diffusion is thermally activated the susceptibility to slow crack growth increases as temperature increases, as shown by the decrease of the exponent N from 10 at 1100 °C to 5 at 1200 °C. These results are complimentary to those found by Milz et al.[14] using a similar range of stressing rates. They reported $N = 18$ and 9.4 at 1000 and 1100 °C, respectively and failure accompanied by extensive microstructural degradation.

When the effects of the external contamination were reduced using bundles of fibres, no silicate intergranular phases or pockets at triple points were detected by TEM in bundles subjected to creep up to 1300 °C. However, the elongated grain growth of the alumina phase in the core of the fibre at 1300 °C during heat treatment without load[3] or during creep result from the formation of thin intergranular films. Calcium and sodium, even at low concentrations, segregate at grain boundaries producing intergranular liquid phase. This mechanism is accentuated by the presence of interfaces of small radii of curvature in the mullite aggregates which increase their solubility.[15] The grain boundaries can be further dewetted during the cooling of the sample. As TEM observations of the fibres tested at 1300 °C were made at room temperature this must explain why no intergranular films were detected. At 1400 °C, intergranular films are observed and the evolution of microstructure of the fibre core depends on the applied stress through a stress enhanced diffusion of the contaminants. For the lowest stresses, this leads to the abnormal grain growth of isolated alumina grains, allowed by long test times and the moderate growth of the majority of the grains. The highest stresses induce an overall grain growth of alumina elongated grains. In these two cases, this growth is oriented in the load direction and results from the preferential growth of the elongated alumina particles already oriented along the fibre axis in the as received fibre.

5.2. Deformation and damage mechanisms in creep

The creep behaviour results from the combination of several microstructural mechanisms, schematised in Fig. 11, in response to time, temperature and loading. At 1200 and 1300 °C the variation of the steady state creep rate $\dot{\varepsilon}$ as function of the applied stress σ (expressed in Pa) and temperature T (in Kelvin) can be fitted with the general expression:

$$\dot{\varepsilon} = A \cdot (\sigma - \sigma_{th})^n \cdot \exp(-Q/RT).$$

with Q, the activation energy for creep, equal to 702 kJ/mol, and the stress exponent n equal to 2. The threshold stress, σ_{th},expresses that positive deformation is only seen above σ_{th} whereas shrinkage occurs below $\sigma_{th.}$. The value of this threshold was determined from experimental tests to be equal to 12 MPa at 1300 °C and 80 MPa at 1200 °C. A is a constant, determined as being 8 s/Pa^2.

The creep activation energy and stress exponent of mullite are strongly dependant on the method of preparation, and the presence or not of intergranular amorphous phases. An activation energy of the order of 700 kJ/mol is typical of a diffusional creep of mullite[16] but this mechanism is associated with a stress exponent of one and samples supposed to be deprived of intergranular silicate phases. The results presented can then more likely be compared to those obtained by Hynes and Doremus on mullite synthetized by a sol gel process with grains of 0.96 μm in size separated by a glassy phase.[17] They report an activation energy of 742 kJ/mol and a stress exponent of 1.6. The creep rates published for these samples are comparable to that found in this study although they do not take into account the presence of elongated alumina grains. The stress exponent of 2, found in this study, is explained by the higher viscosity of the thinner alumino-silicate intergranular phase. Even if the viscosity of the silicate phase is lowered by the presence of aluminium, calcium and sodium, it increases dramatically when the thickness of the film decreases to be of the order of a few SiO_4 tetrahedra due to a local ordering of the tetrahedra in the immediate vicinity of the grains[18] so that Newtonian behaviour breaks down.[19]

At 1400 °C the dissolution rate of mullite and the thickness of the intergranular films are increased giving rise to strain rates proportional to the applied stress. Grains slide in this fluid phase of low viscosity which is squeezed to the outer regions of the fibres. The diffusion of aluminium ions in the liquid phase and reprecipitation of these ions on alumina grains induce their concomitant

growth in the tensile axis direction. It was not felt justified to extract and interpret activation energies from these data for the creep mechanisms at 1400 and 1500 °C. The steady state creep equations assume no evolution of the microstructure during secondary creep which was not the case at these temperatures. Despite the exsolution of the creep resistant mullite and the presence of thin silicate intergranular films, the growth of elongated alumina grains in the load direction is responsible for lower creep rates than for isotropic fine grain alumina systems. Theoretical calculations of creep rates by a dissolution reprecipitation mechanism, in structures made of grains having an aspect ratio of λ oriented in the tensile axis and separated by a thin glassy phase show a decrease of the creep rate by a factor $(1+\lambda)$ because of an increase of the diffusion paths.[20]

Damage associated with moderate grain growth is due to the development of microcracks from regions of non accommodated sliding. These cracks propagate intergranularly and cause failure, either by their coalescence or by the catastrophic failure of the remaining section. Such failures are seen at 1200 and 1300 °C for all the stress ranges studied and at 1400 °C at intermediate loads. The overall larger grain growth or abnormal growth of isolated grains give rise to catastrophic failures from grains reaching the critical defect size or growing intergranular cavities. Such a failure mode is seen for both low and high loads at 1400 and at 1500 °C for all loads studied.

5.3. Comparison with other oxide fine fibres

The Nextel 720 fibre is produced by the spinning of a gel and a rapid pyrolysis leading to high interfacial energies and high reactivity. This, added to the ability of mullite to dissolve in the presence of alkaline contaminants induces microstructural instability under load, which has also been described by other authors and under other experimental conditions.[14] Such instability has not been seen for monophase pure α-alumina fibres or spinel alumina in silica (Altex or Nextel 440 fibres or mullite fibres (Nextel 480) using the same experimental procedures as those used in this study.[21] The combination of alumina and mullite appears not to be favourable in terms of microstructural stability as the reprecipitation of alumina from the dissolving mullite increases the concentration of the alkaline containing silicate phase and the dissolution rate of mullite. On the other hand single phase polycristalline mullite fine fibres give rise to low strengths due to large grains and the dispersion of a second phase into mullite impedes mullite grain growth. If a two phase fibre is required a mullite zirconia fibre could be a better candidate, in terms of microstructural stability, as in this case mullite instead of alumina reprecipitates from the liquid phase formed.[22,23] Despite its high alkaline sensitivity, the Nextel 720 fibre exhibits the highest creep resistance off all commercial fine oxide fibres. The creep rates at 1300 °C are reduced by three orders of magnitude when compared to pure alpha alumina fibres with isotropic fine grain structures, which exhibit superplastic behaviour (Fibre FP, Nextel 610). The excellent creep resistance of the Nextel 720 fibre can be attributed first to the inherent creep resistance of mullite but also to the gradual evolution of its microstructure toward oriented elongated alumina grains and this despite the presence of thin silicate intergranular films.

5.4. Conclusion

The combination of sub-micron mullite and alumina grains in the presence of alkalis leads to specific tensile and creep behaviour and microstructural modifications which are different from those of single phase mullite or alumina systems.

1. From 1100 °C, in tension, cracks nucleate around surface flaws by the stress enhanced diffusion of alkalis. Mullite dissolution, liquid phase formation and alumina growth occur around the crack tip giving rise to subcritical crack growth. Fast alumina grain growth with rates of the order of 1 μm/s at 1200 °C is seen in the regions of the crack initiation.
2. If fast surface grain growth can be suppressed by a reduction of external contamination, creep life times can reach several hours at 1500 °C.
3. During creep, mullite is progressively dissolved to form an alumino-silicate phase which partially reprecipitates into alumina. The alkalis dissolved in the liquid phase increase the interfacial reaction rate and make the alumina basal plane the lowest energy plane. Deformation occurs by grain boundary sliding through the liquid phase and by the preferential growth of oriented elongated alumina particles present in the as received fibre. The fibre is progressively converted into elongated alumina grains with long flat (0001) interfaces parallel to the tensile axis and a silicate phase rejected toward the outside of the fibre.
4. At a given temperature, the stress enhanced diffusion of alkalis results in mullite dissolution and alumina growth both of which increase with an increase of applied stress. From 1400 °C abnormal alumina grain growth is seen at low stresses whereas higher stresses give rise to normal grain growth.
5. Failure in creep occurs, either after damage accumulation by the coalescence of several intergranular microcracks, if grain growth is restricted, or catastrophically from large growing grains or cavities. The corresponding fracture morphologies differ with the former being intergranular and non planar and the latter mostly intragranular and planar.

References

1. Lavaste, V., Berger, M. H., Bunsell, A. R. and Besson, J., Microstructure and mechanical characteristics of alpha alumina-based fibres. *J. Mater. Sci.*, 1995, **30**, 4215–4225.
2. Wilson, D. M., Lieder, S. L. and Lueneburg, D. C., Microstructure and high temperature properties of Nextel 720 fibers. *Ceram. Eng. Sci. Proc.*, 1995, **16**(5), 1005–1014.
3. Deleglise, F., Berger, M. H., Jeulin, D. and Bunsell, A. R., Microstructural stability and mechanical properties of Nextel 720 the fibre. *J. Eur. Ceram. Soc.*, 2001, **21**, 569–580.
4. Berger, M. H. and Bunsell, A. R., Thin foil preparation of small diameter ceramic or glass fibres for observation by TEM. *J. Mater. Sci.*, 1993, **12**, 825–828.
5. Hagege, R. and Bunsell, A. R., Testing methods for single fibres. In *Fibre Reinforcements for Composite Materials, Composite Materials Series 2*, ed. A. R. Bunsell. Elsevier, Amsterdam, 1988.
6. Hay, R. S., Boakye, E. E., Petry, M. D., Berta, Y., Von Lehmden, K. and Welch, J., Grain growth and tensile strength of 3M Nextel 720 after thermal exposure. *Ceram. Eng. Sci. Proc.*, 1999, **20**(3), 153–163.
7. Petry, M. D. and Mah, T. I., Effect of thermal exposure on the strengths of Nextel 550 and 720 filaments. *J. Am. Ceram. Soc.*, 1999, **82**(10), 2801–2807.
8. Wiederhorn, S. M., Subcritical crack growth in ceramics. In *Fracture Mechanics of Ceramics*, ed. R. C. Bradt, D. P. H. Hasselman and F. F. Lange. Plenum Press, New York, 1974, pp. 613–646.
9. Wilson, D., private communication.
10. Song, H. and Cobble, R. L., Origin and growth kinetics of platelike abnormal grains in liquid phase-sinterd alumina. *J. Am. Ceram. Soc.*, 1990, **73**(7), 2077–2085.
11. Baudin, C. and Villar, M. P., Influence of thermal aging on microstructural development of mullite containnig alkalis. *J. Am. Ceram. Soc.*, 1998, **81**(10), 2741–2745.
12. Baudin, C., Fracture mechanisms in a stoichiometric $3Al_2O_3$2-SiO_2 mullite. *J Mater Sci.*, 1997, **32**, 2077–2086.
13. Yu, H. H. and Suo, Z., Delayed fracture of ceramics caused by stress-dependent surface reactions. *Acta Mater.*, 1999, **47**(1), 77–88.
14. Milz, C., Goering, J. and Schneider, H., Mechanical and microstructural properties of Nextel 720 relating to its suitability for high temperature application in CMCs. *Ceram. Eng. Sci. Proc.*, 1999, **20**(3), 191–198.
15. Thomson-Freundlich, In *Physical Ceramics*, ed. Y.-M. Chiang, D. B. Birnie and W. D. Kingery. John Wiley & Sons, New York, 1997, p. 356.
16. Lessing, P. A., Gordon, R. S. and Mazdiyasni, K. S., Creep of polycrystalline mullite. *J. Am. Ceram. Soc.*, 1975, **58**(34), 149.
17. Hynes, A. P. and Doremus, H., High-temperature compressive creep of polycrystalline mullite. *J. Am. Ceram. Soc.*, 1991, **74**(10), 2469–2475.
18. Horn, R. G. and Israelachvili, J. N., *Chem. Phys. Letters*, 1980, **71**(2), 192–194.
19. Smolej, V., Comment on ''liquid phase sintering: are liquids squeezed out from between compressed particles?''. *J. Am. Ceram. Soc.*, 1983, **66**(2), C–33.
20. Wilkinson, D. S., Creep mechanisms in multiphase ceramic materials. *J. Am. Ceram. Soc.*, 1998, **81**(2), 275–299.
21. Berger, M. H., Lavaste, V. and Bunsell, A. R., Properties and microstructure of small diameter alumina based fibers. In *Fine Ceramic Fibers*, ed. A. R. Bunsell and M. H. Berger. Marcel Dekker, 1999, p. 111.
22. Deléglise, F., PhD thesis, Ecole des Mines de Paris, France, 5 July 2000.
23. Lewis, M. H., York, S., Freeeman, C., Alexander, I. C., Al-Dawery, I., Butler, E. G. and Doleman, P. A., Oxide CMCs; novel fibres, coatings and fabrication procedures. *Ceram. Eng. Sc. Proc.*, 2000, **21**(3), 535–574.